Low Temperature Physics/Fizika Nizkikh Temperatur, 2015, v. 41, No. 11, pp. 1206–1208

Short notes

Charge-ordering induces magnetic axes rotation in organic materials $(TMTTF)_2X$ (with X = SbF_6, AsF_6, and PF_6)

C.-E. Dutoit[1], S. Bertaina[1], M. Orio[2], M. Dressel[3], and A. Stepanov[1]

[1]*Aix-Marseille Université, CNRS, IM2NP UMR 7334, 13397 cedex 20, Marseille, France*
E-mail: anatoli.stepanov@im2np.fr

[2]*Aix-Marseille Université, CNRS, Centrale Marseille, ISM2 UMR 7313, 13397 Marseille, France*

[3]*Physikalisches Institut, Universität Stuttgart, 70550 Stuttgart, Germany*

Received July 2, 2015, published online September 25, 2015

We have performed a comprehensive EPR investigation of the quasi-one-dimensional organic systems $(TMTTF)_2X$ with centrosymmetrical anions X (X = SbF_6, AsF_6, and PF_6). We observe a strong rotation of *g*-factor principal axes when the temperature decreases below charge-ordering temperature T_{CO}. The possible origin of this rotation is analyzed on the basis of quantum chemical calculations performed using density functional theory method. A good agreement between theory and experiment is found.

PACS: **71.27.+a** Strongly correlated electron systems; heavy fermions;
75.85.+t Magnetoelectric effects, multiferroics;
76.30.–v Electron paramagnetic resonance and relaxation.

Keywords: organic salt, electron paramagnetic resonance, charge ordering, loss of the symmetry centre.

Quasi-one-dimensional systems such as organic charge-transfer salts have been intensively studied during the last decades. Among these organic salts, $(TMTTF)_2X$ molecules, where X represent a inorganic anion, exhibit a very rich phase diagram [1] and display phase transitions such as antiferromagnetic, charge-ordering, spin-Peierls, etc. They cristallize in the triclinic $P\bar{1}$ space group with two donor molecules and one anion in the unit cell. TMTTF molecules are arranged in a "zig-zag" configuration, forming stacks along the **a** direction and layers in **ab** plane which alternate with the anion X along the **c** axis. Charge-ordering (CO) is observed in these compounds at T_{CO} = 65 K, 105 K [2], and 154 K [3] for X = SbF_6, AsF_6, and PF_6, respectively.

Here, we report a continuous wave (cw) electron paramagnetic resonance (EPR) study of $(TMTTF)_2X$ (X = SbF_6, AsF_6, and PF_6). The rotation of *g*-factor principal axes was observed in these three salts when the temperature decreases from 300 to 4 K. This rotation is considerably enhanced below the charge-ordering transition. We discuss the possible origin of this rotation by comparing experimental results with those obtained from our quantum chemical calculations performed with density functional theory (DFT). When considering only a thermal contraction of the TMTTF structure, as temperature decreases, the DFT calculations show a rotation of about 4–5° between T = 300 and 4 K. But when a uniform anion displacements due to the charge-ordering transition were considered [4] we obtain a much stronger rotation ranging up to 26° in the case of $(TMTTF)_2SbF_6$ salt, in fair agreement with the experimental data.

Single crystals of $(TMTTF)_2X$ were prepared by standard electrochemical method [5] and were needle-shaped with typical dimensions of 3×0.1×0.5 mm. X-band EPR measurements were performed on a cw Bruker EMX spectrometer operating at about 9.6 GHz and equipped with a continuous flow cryostat covering the temperature range from 4 to 300 K. The microwave power supplied into the cavity was below 1 mW in order to avoid saturation of the EPR signal. The modulation frequency was set at 100 kHz and its amplitude was chosen between 0.1 and 1 G to prevent distortion of the EPR signal due to over-modulation. The sample was fixed on quartz suprazil rod with the **a** axis parallel to the rotation axis, in addition the **a** direction

being oriented along the microwave magnetic field $\mathbf{h}_{mw}$. A small amount of DPPH was used as *g*-factor marker. The sample holder was rotated around the **a** axis every 5° with an accuracy of 0.25°. For each set of measurements a fresh crystal was used.

Quantum chemical calculations have been performed by DFT method using the ORCA program package [6]. The *g* factor was obtained from single point calculations, combing the hybrid functional B3LYP [7,8] and the EPR-II basis set, as a second derivative property of the energy with respect to the external magnetic field and the electron magnetic moment [9–12]. To analyze our experimental results, we have introduced an orthogonal coordinate system with $\mathbf{a}^*$, $\mathbf{b}^*$, and $\mathbf{c}^*$ axes such as $\mathbf{a}^*$, $\mathbf{b}^*$, and $\mathbf{c}^*$ are the principal axes of the *g* factor. We choose the $\mathbf{a}^*$ axis of our coordinate system to be parallel to the long axis of the studied crystal which according to [13] is parallel to the crystallographic **a** axis. Independently, by EPR measurements, we have checked that the $\mathbf{a}^*$ axis is one of the principal axes of the *g* factor. Therefore, the two other *g*-factor principal axes should be in the plane perpendicular to the $\mathbf{a}^*$ axis, and are denoted $\mathbf{b}^*$ and $\mathbf{c}^*$ axes. Note that the $\mathbf{b}^*$ and $\mathbf{c}^*$ axes are not fixed by the symmetry elements of the point group in considered low symmetry crystals.

Figure 1 shows a representative angular dependence of the *g* factor in the $\mathbf{b}^*\mathbf{c}^*$ plane taken at different temperatures for $(TMTTF)_2SbF_6$ sample. We observe a clear *g*-factor anisotropy which is in agreement with previous results [13]. We assign the minimum of *g*-factor value in $\mathbf{b}^*\mathbf{c}^*$ plane to the $\mathbf{b}^*$ axis and the maximum to the $\mathbf{c}^*$ axis. To simplify our analysis the room temperature (RT) curve of $g(\theta)$ is chosen as a reference and we set the magnetic field orientation $\mathbf{H} \| \mathbf{b}^*$ as $\theta = 0°$ in the laboratory coordinates at 300 K.

Our main finding is that the $\mathbf{b}^*$ axis *continuously rotates* when the temperature decreases. For instance, as seen in Fig. 1, the position of the $\mathbf{b}^*$ axis is close to $\theta = 19°$ in $(TMTTF)_2SbF_6$ at $T = 30$ K. This difference in the $\mathbf{b}^*$ axis position is denoted $\Delta\theta(T)$ and is plotted in Fig. 2.

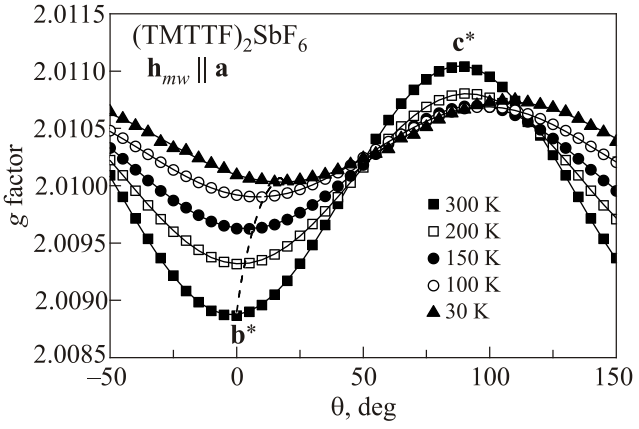

Fig. 1. A representative *g*-factor angular dependence for $(TMTTF)_2SbF_6$ at different temperatures when the static magnetic field is applied perpendicular to the **a** axis. The evolution of the position of the g_{b^*} is indicated by a dashed line.

Interestingly, the $\Delta\theta$ temperature dependence is not monotonic, and is characterized by two different behaviors in two distinct temperature intervals. Between RT and T_{CO}, $\Delta\theta$ reaches at most 5–6° with a slow variation. In contrast, between T_{CO} and 4 K, the $\Delta\theta$ temperature dependence is much more important, and at low temperature the $\Delta\theta$ reaches up to 22° for $(TMTTF)_2SbF_6$. This latter behavior can be attributed to charge-ordering phase transition.

To explain the observed rotation calculations were performed using experimental crystal data obtained at different temperatures from previous studies [14,15] as input parameters. They were conducted to compute the *g*-factor parameters and the corresponding spin density distributions. Above T_{CO}, the charge is equally distributed between two neighbouring TMTTF molecules. Below T_{CO}, there is a charge disproportion between two TMTTF molecules causing the loss of the symmetry centre.

In Fig. 2 in addition to the observed temperature dependence of $\Delta\theta$ we show the one predicted by DFT calculations. Consistently with experiments, the calculations

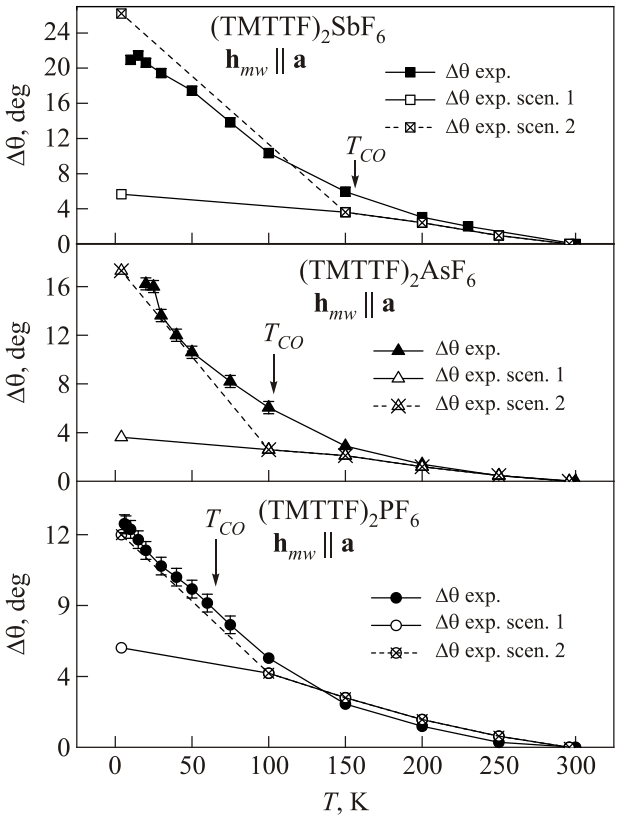

Fig. 2. Experimental temperature dependence of the $\mathbf{b}^*$ axis position as compared to its position at RT for $(TMTTF)_2X$ (X = = SbF_6, AsF_6, and PF_6). The calculated $\mathbf{b}^*$ axis position due to the thermal contraction of TMTTF is represented by $\Delta\theta$ calc. scen. 1 and due to the thermal contraction of TMTTF and uniform anion displacements is represented by $\Delta\theta$ calc. scen. 2.

reveal two different behaviors of $\Delta\theta(T)$ in two distinct temperature intervals. When considering only thermal contraction of the molecular structure between 300 K and T_{CO}, $\Delta\theta_{calc}(T)$ varies slowly up to 4–5° as temperature decreases (scenario 1). If now one considers a uniform anion displacement of about 10% towards the charge rich TMTTF [4,16] below T_{CO}, $\Delta\theta_{calc}(T)$ reaches up to 26° for $(TMTTF)_2SbF_6$ (scenario 2), 18° for $(TMTTF)_2AsF_6$ and 12° for $(TMTTF)_2PF_6$, respectively, in a good agreement with experiment.

In conclusion, quasi-one-dimensional charge-transfer salts $(TMTTF)_2X$ with X = AsF_6, PF_6, and SbF_6, have been studied by cw X-band EPR and data have been interpreted by quantum chemical calculation. We observed the *g*-factor principal axes rotation when the temperature decreases. To explain this behavior, quantum chemical calculations were performed using the DFT method. Our computational study has revealed two distinct temperature behaviors of $\Delta\theta$ in a good agreement with experimental results. We argue that the charge-ordering transition in $(TMTTF)_2X$ crystals induces a strong *g*-factor axis rotation around the **a** axis.

This work was supported by CNRS's research federation RENARD (FR3443) for EPR facilities.

1. D. Jérome, *Science* **252**, 1509 (1991).
2. D. Chow, F. Zamborszky, B. Alavi, D. Tantillo, A. Baur, C. Merlic, and S. Brown, *Phys. Rev. Lett.* **85**, 1698 (2000).
3. P. Monceau, F.Y. Nad, and S. Brazovskii, *Phys. Rev. Lett.* **86**, 4080 (2001).
4. P. Foury-Leylekian, S. Petit, G. Andre, A. Moradpour, and J. Pouget, *Physica B*: *Condens. Matter* **405**, S95 (2010).
5. L. Montgomery, *Organic Conductors*, J.-P. Farge (ed.), Marcel, New York (1994).
6. F. Neese, *Wires. Comput. Mol. Sci*. **2**, 73 (2012).
7. A.D. Becke, *J. Chem. Phys.* **98**, 1372 (1993).
8. C. Lee, W. Yang, and R.G. Parr, *Phys. Rev. B* **37**, 785 (1988).
9. S. Koseki, M.S. Gordon, M.W. Schmidt, and N. Matsunaga, *J. Phys. Chem*. **99**, 12764 (1995).
10. S. Koseki, M.W. Schmidt, and M.S. Gordon, *J. Phys. Chem*. **96**, 10768 (1992).
11. F. Neese, *J. Chem. Phys.* **118**, 3939 (2003).
12. F. Neese, *J. Chem. Phys.* **115**, 11080 (2001).
13. S. Yasin, B. Salameh, E. Rose, M. Dumm, H.-A. Krug von Nidda, A. Loidl, M. Ozerov, G. Untereiner, L. Montgomery, and M. Dressel, *Phys. Rev. B* **85**, 144428 (2012).
14. K. Furukawa, T. Hara, and T. Nakamura, *J. Phys. Soc. Jpn.* **78**, 104713 (2009).
15. T. Granier, B. Gallois, L. Ducasse, A. Fritsch, and A. Filhol, *Synth. Met*. **24**, 343 (1988).
16. M. de Souza, P. Foury-Leylekian, A. Moradpour, J.-P. Pouget, and M. Lang, *Phys. Rev. Lett.* **101**, 216403 (2008).